Hydrogeology and Geochemistry of Near-shore Submarine Groundwater Discharge at Flamengo Bay, Ubatuba, Brazil

June A. Oberdorfer (San Jose State University)
Matthew Charette, Matthew Allen (Woods Hole Oceanographic Institution)
Jonathan B. Martin (University of Florida) and
Jaye E. Cable (Louisiana State University)

Abstract: Near-shore discharge of fresh groundwater from the fractured granitic rock is strongly controlled by the local geology. Freshwater flows primarily through a zone of weathered granite to a distance of 24 m offshore. In the nearshore environment this weathered granite is covered by about 0.5 m of well-sorted, coarse sands with sea water salinity, with an abrupt transition to much lower salinity once the weathered granite is penetrated. Further offshore, low-permeability marine sediments contained saline porewater, marking the limit of offshore migration of freshwater. Freshwater flux rates based on tidal signal and hydraulic gradient analysis indicate a fresh submarine groundwater discharge of 0.17 to 1.6 m^3/d per m of shoreline. Dissolved inorganic nitrogen and silicate were elevated in the porewater relative to seawater, and appeared to be a net source of nutrients to the overlying water column. The major ion concentrations suggest that the freshwater within the aquifer has a short residence time. Major element concentrations do not reflect alteration of the granitic rocks, possibly because the alteration occurred prior to development of the current discharge zones, or from elevated water/rock ratios.

Introduction

While there has been a growing interest over the last two decades in quantifying the discharge of groundwater to the coastal zone, the majority of studies have been carried out in aquifers consisting of unlithified sediments or in karst environments. This study is part of an intercomparison experiment that examines a range of techniques used to quantify submarine groundwater discharge (SGD) in a fractured-rock aquifer environment. This is a difficult environment to evaluate due to the spatial variability in aquifer properties resulting from the variability in the spacing, aperture, and interconnectedness of the fractures. While the intercomparison experiment examines SGD on a variety of scales, the work reported on here quantifies SGD on the small scale of a beach transect in the near-shore region where much of the discharge is expected to take place. Previous SGD studies (Harvey and Odum, 1990; Vanek,

1993; Nuttle and Harvey, 1995; Staver and Brinsfield, 1996; Robinson, 1996) have been carried out on a small scale (tens to hundreds of meters), while previous SGD intercomparison experiments (Burnett et al., 2002) have examined SGD on multiple scales, including the local scale.

The study area is located in the Pre-Cambrian shield region of eastern Brazil. Groundwater occurs in fractures in the granitic and metamorphic rocks of the area. Not a great deal is known about the groundwater in the fractured bedrock since it is not used to a significant degree as a resource. There is some utilization of localized springs related to major fractures. The region is one of the highest rainfall regions of Brazil (Rebouças, 2002) which means recharge is likely to occur readily.

Understanding SGD on this small scale should provide insight into data collected on the much larger scale of some of the geochemical tracer studies that were being carried out at the same time. This study also documents groundwater discharge in a geologic environment that was poorly documented previously. The location of the field area is given in Figure 1. Enseada de Flamengo (Flamengo Bay), near Ubatuba, São Paulo state, is the location of the marine laboratory of the University of São Paulo. The beach at the marine laboratory was selected for in-depth studies because of the presence of weathered bedrock and sediment above the fractured granite; this granular material permitted the installation of wells and equipment that would not have been possible to install in fresh, fractured bedrock.

Methods

Piezometer Installation. Eleven small-diameter (5 cm), shallow wells were installed by a Brazilian consulting company (Gea) in October 2001. Two of the wells were installed in the

inter-tidal zone but were subsequently destroyed prior to the start of the experiment. The locations of the remaining nine wells are shown in Figure 2. Well 0 was completed at a depth of 5.0 m below ground surface (bgs), while the depth of completion of the remaining wells ranged from 0.7 to 2.1 m bgs. These wells were hand-augered and completed with perforated PVC pipe with plastic screen clamped around the perforated section to minimize seepage of sediment into the wells. During installation of the onshore wells (wells 0, A1 and B1), augering had to stop when geologic materials too hard to auger through by hand were encountered. For the wells completed offshore, all well-casings extended well above the high tide level.

Coring. Sediment cores were collected at the location of the two WHOI wells (WH1 and WH2). Ten cm diameter aluminum irrigation tubing was driven into the sediment using a slide hammer and recovered with a makeshift tripod and come-along. Core 1 (located at well WH2) was approximately 190 cm long and core 2 (well WH1) was 100 cm. The cores were extruded onto plastic sheeting and the sediment characteristics were logged in ~13 cm intervals.

Water Level Measurements. Water levels in the wells were measured manually with an electric well sounder. Water levels were measured and recorded at well 0 and a stilling well on the adjacent marine laboratory dock using an *Infinities USA Inc.,* ultrasonic electronic water level data logger.

Slug/Bail Tests. The slug/bail tests were performed by either bailing (wells 0 and B1) or pumping (wells A2, A3, B2, B3) the well to lower the water level followed by monitoring of the water level recovery. In the case of the two bailed wells, the bailed water was later reintroduced into the well to cause a water level rise, and the recovery to the original level was monitored. Offshore wells (A2, A3, B2, B3) were pumped using a GeoTech peristaltic pump. In all cases, water levels were recorded manually and replicate field tests were performed whenever possible

on each well. The data from the slug/bail tests was analyzed using the method of Hvorslev (1951) to obtain effective hydraulic conductivity of the sediments surrounding these wells.

Tidal Signal Analysis. Bay and well 0 water level data were collected for approximately one week. These data were analyzed for tidal lag (time between maximum or minimum water levels in the ocean and corresponding maximum or minimum water levels in the well) and tidal efficiency (ratio of water level change in the well to that in the ocean over a half tidal cycle). These values were used to calculate the hydraulic conductivity of the aquifer (Jacob, 1950).

Mini-wellpoint Sampling for Salinity. Small diameter (1 cm) metal wellpoints, perforated over a 2 cm interval near the pointed tip, where hand pushed into the sediment to depths of up to 1 m. Porewater was sampled by purging the wellpoint of 250 ml of water, followed by collecting of a 100 ml water sample. The salinity of each water sample was read on a refractometer.

Water Quality Sampling and Analysis. Porewater from the two WHOI wells (WH1 and WH2) was collected using a direct-push, shielded-screen piezometer (AMS, Inc. Madison, Wisconsin USA). Samples were collected at 15 or 30 cm intervals using a peristaltic pump coupled with Teflon tubing. At each interval, salinity and other ancillary water quality properties were measured with a YSI 600R multi-probe mounted in a flow-through cell. After several volumes of the tubing were flushed, filtered samples for nutrient determination were collected and stored frozen until analysis. Back in the laboratory, nutrient samples were thawed and run on a Lachat QuickChem 8000 flow injection analyzer using standard colorimetric techniques.

Four multisamplers (multi-level piezometers; Martin et al., 2003) were installed in a transect extending approximately 30 meters offshore. The multisampler closest to shore (MS-2) was located 2.5 m from the low tide line, and the remaining three multisamplers MS-5, MS-3,

and MS-4 were installed at distances of 6.5, 10.5 and 26.5 m from the low tide line. All multisamplers were installed to depths of 230 cm below the seafloor, but only the two farthest offshore yielded water from all eight ports; water could not be pumped from the lowest three ports of MS-2 and the lowest two ports from MS-5. One multisampler per day was sampled between November 16 and November 20, 2003. Water was initially pumped from MS-3 on November 17, 2003 and then again on November 18, 2003 as a comparison with the previous sampling time. No samples were collected when it was pumped the second time, but field parameters (salinity, DO, and pH) were measured.

Waters from all multisamplers were measured for salinity, DO, and pH at the time they were pumped. When values of these field parameters were stable, water samples were collected in 30 ml Nalgene HDPE bottles. Two bottles were collected, one was filtered and acidified, and the other was collected as a raw sample. Chloride concentrations of the water was measured by titration with $AgNO_3$. Sodium and potassium concentrations were measured with ion chromatography.

Results

Hydrogeologic Conceptual Model. The hydrogeology in the immediate vicinity of the marine laboratory was studied using geologic descriptions made during the installation of the nine wells at the site, through excavations along the beach, via cores sampled in the area of the two transects, and during installation of pore water samplers offshore. Onshore, the geologic materials consisted of about 3 m of colluvial material overlying highly weathered, granitic bedrock (to the total depth of the boring for well 0 at 5 m). Along the beach (wells A1 and B1 and the two destroyed wells, located near the low tide line) about 1 m of sand was found to

overlie granitic boulders that made well installation difficult. In the nearshore submerged region, deposits consisted of about 0.5 m of coarse sand overlying about 0.3 m of hard sand with gravel, organics, and fines (Figure 3) sitting atop highly weathered bedrock. About 24 m offshore there was a fairly abrupt transition to fine marine sediment over 2 m thick. A hydrogeologic cross-section is given in Figure 4.

Sediment cores recovered revealed a thin layer (~0.5 - 2 m) of sediment on top of deeply weathered crystalline bedrock. Most of the sediments, excluding the nearshore surface samples, were very poorly sorted. From the two recovered cores, most intervals contained a small amount of sand, silt, clay, and shell hash. In the offshore core (core 1) the silts and clays throughout were low permeability making this location a poor conduit for SGD. In the nearshore core 2, the surficial sediments were extremely coarse grained and had been well sorted, presumably by wave action. The transition from well-sorted coarse sands to poorly sorted sands, silts and clays is shown in Figure 3.

Slug Testing. Slug tests were performed on well 0, completed in the weathered bedrock, and well B1, completed in sand among boulders. The results for the slug and bail tests on well 0 gave an average hydraulic conductivity for the weathered granitic bedrock of 1.0×10^{-4} cm/s (0.09 m/d). The results for the slug and bail tests on well B1 yielded an average hydraulic conductivity for the sandy beach material of 2.9×10^{-3} cm/s (2.5 m/d). Offshore wells yielded effective hydraulic conductivities of about 1.1×10^{-3} cm/s (0.9 m/d) to 5.2×10^{-3} cm/s (4.5 m/d). Well transect B demonstrated a higher overall hydraulic conductivity than transect A, despite being separated by only about 30 m alongshore (Table 1).

Tidal Signal. Relative changes in water levels for Flamengo Bay and well 0 are presented in Figure 5. The average (n = 8, for data of acceptable quality) tidal lag was 14.2 ± 1.5 hours and

the average (n = 6) tidal efficiency was 0.095 ± 0.033. Assuming an aquifer thickness of 3 m (the saturated weathered bedrock and colluvium) and a specific yield for the aquifer of 0.20, a hydraulic conductivity of 6.1 x 10^{-3} cm/s (5.3 m/d) was calculated from the tidal lag. The hydraulic conductivity calculated from the tidal efficiency was 5.6 x 10^{-2} cm/s (49 m/d).

Darcy's Law Estimates of SGD. The hydraulic gradient on land was measured between wells 0 and B1. With a water level change of 0.13 m over a distance of 12.3 m, the hydraulic gradient was calculated to be 0.011, representing a single snapshot of the gradient at that particular moment. This gradient will change at different times in the tidal cycle as the tidal signal is propagated inland. The hydraulic gradient could vary with time by a factor of two from the value given.

It is possible to calculate the discharge of freshwater per unit width of shoreline using Darcy's Law:

$Q/w = -K\ b\ dh/dl$

where

Q: discharge ($L^3\ T^{-1}$)

w: width of shoreline (L)

K: hydraulic conductivity ($L\ T^{-1}$)

b: aquifer thickness (L)

dh/dl: hydraulic gradient ( )

The aquifer thickness was again taken as approximately 3 m. A range of hydraulic conductivity values has been determined. These values were used to estimate discharge along the shoreline (Table 1).

The calculated freshwater SGDs vary over almost four orders of magnitude. The most reliable estimate of hydraulic conductivity is from the tidal signal propagation data, which averages the permeability over a large volume of aquifer material and provides a more integrated temporal estimate as well. The slug/bail tests provide more of a point measurement and can be sensitive to the well completion and testing methods. It was necessary to assume a specific yield value and aquifer thickness to analyze the tidal data, so uncertainties in those assumptions create uncertainties in the hydraulic conductivity value determined from that method. However, the lower estimate of fresh SGD using the tidal signal approach is similar to values from the bail/slug tests on offshore (surf zone) well sediments, thus, lending credence to the tidal signal approach.

Water Quality. Mini-wellpoints were used at the multiple locations to evaluate groundwater salinity distributions. The salinity was high in the coarse-grained sand and dropped abruptly once the hard, fine-grained layer was penetrated (Figure 6). Data from the multi-level piezometers revealed a thin fresh water lens present in near-shore sediments about 11 m from the low tide line (Figure 7). This tongue of freshwater moved within 40 cm of the sediment-water interface at about 8 m offshore (low tide baseline). The freshwater lens was thin and apparently confined by a hard layer to about 1.5 m below the sediments as it moved farther offshore.

Groundwater profiles were also collected for salinity and nutrients at piezometers WH1 and WH2 (Figure 2). The salinity of the groundwater at WH1 above the coarse-fine sediment transition was approximately 29-30 (Fig. 8a). The groundwater immediately below the transition was in the range of 0-2. Groundwater at this location appeared to be a net source of nutrients to the overlying water column. In particular, dissolved inorganic nitrogen (DIN) ranged from 5-20 μM in the groundwater compared with less than 1 μM in the surface waters (Fig. 8a). Silicate

was also highly enriched in the groundwater, ranging from 30 to 120 μM. Due to this sharp salinity and porosity gradient, neither of the core locations appeared to be zones of high SGD. The piezometer profile at WH2 revealed (Fig. 8b) relatively constant salinity throughout the upper 1.2 m of sediment. DIN was slightly higher on average (up to ~25 μM) but generally decreased with depth suggesting the sediments were a sink for DIN (e.g., denitrification). Silicate concentrations were similar to the nearshore profile but also decreased with depth. Below 1.2 m depth the piezometer encountered a hard layer which could not be penetrated.

Dissolved oxygen and pH results from the multi-level piezometers are presented in Figure 9. The dissolved oxygen concentration decrease with depth in the pore water, but are never completely depleted, remaining between approximately 1 and 3 mg/L. Dissolved oxygen was measured in an open sampling cup and the measured oxygen could reflect an artifact of oxygen contamination of the sample. Alternatively, oxygen in the pore waters could reflect the lack of an electron acceptor in these organic-poor sediments. pH values also decrease in the sediment, with the strongest gradients decreasing to a low value of around 5 at the two near-shore sites MS-2 and MS5. The pH profiles mimic the salinity profiles (e.g. Fig. 7) with lower pH occurring in the low salinity water. Na/Cl molar ratio and K/Cl molar ratio versus pH for the same four multi-piezometer stations are presented in Figure 10. This figure demonstrates that Na/Cl and K/Cl ratios of the low pH and low salinity water differ from seawater values as measured in the overlying water column. In addition, the two ratios differ from each other. The Na/Cl ratio is both elevated and depleted relative to seawater value, while the K/Cl ratio is always lower than seawater value. Assuming that salinity and Cl concentrations are conservative in this system, the variations in pH, K and Na concentrations may reflect mixing between the

fresh water end member and seawater, and/or weathering reactions of the granitic rocks and sediments of the region.

Discussion

The geology at this site appears to exert a strong control on the distribution and discharge of freshwater. Water flows from the land through the weathered granite beneath the hard layer that separates the overlying coarse-grained sand from the underlying weathered material. This hard layer appears to restrict downward mixing of the saline water while allowing some upward seepage of the freshwater. The freshwater is again impeded from flowing further offshore where the coarse sand and hard layer end (about 24 m offshore) and the low-permeability, fine-grained, marine sediments begin (Figure 4).

The most reasonable estimate of freshwater SGD, based on the hydraulic conductivity values determined from the tidal signal propagation, range over an order of magnitude from 0.17 to 1.6 m^3/d per m of shoreline. While the freshwater SGD is probably not evenly distributed across the 24 m of coarse sediment nearest shore, an estimate of the average seepage rate can be made by dividing the SGD by that 24 m distance. The net, upward, freshwater seepage rate thus estimated is 7.1×10^{-3} to 6.7×10^{-2} m/d. Salinity in the pore waters along the multi-level piezometer transect shows freshwater from the surficial aquifer flows seaward. While the lateral offshore extent of freshwater is likely heterogeneous, it appears that fresh SGD may discharge nearshore about 8 m from shore (using low tide as baseline) (*see MS5*, Fig. 7). Further offshore along that transect the freshwater lens is downward-dipping, perhaps confined by a hard clay layer, as suggested from sediments core collected during the study. An alternate explanation for the profile in MS5 is that slower upward velocities in the distal portion of the discharge zone

may allow greater exchange across the sediment-water interface through diffusion or by mechanisms such as wave and tidal pumping or bioirrigation (e.g. Martin et al., 2004).

This groundwater seepage rate can be used to estimate the DIN flux to surface waters. If we assume a fresh groundwater DIN endmember of 12 μM (12 mmol m^{-3}), the fresh SGD-derived DIN flux would range between 0.09-0.80 mmol N m^{-2} d^{-1}. These values are nearly an order of magnitude lower than estimates of SGD-derived DIN flux for Chesapeake Bay (Charette and Buesseler, 2004) or South Carolina (Krest et al., 2000), suggesting that nutrient inputs to this region may not be dominated by the subsurface pathway. However, these estimates include brackish to saline SGD, hence our DIN flux may be an underestimate of the total SGD-derived flux to this embayment.

The relatively high dissolved oxygen content (Figure 9) suggests that there is little regeneration of organic matter in the sediments, which could contribute to the smaller flux of DIN compared with Chesapeake Bay and South Carolina, where sedimentary organic matter is more concentrated. The lowest DO concentrations occurs in MS-4 offshore where there is no influence of fresh water discharge. The elevated oxygen concentrations in the other three multisamplers suggest that the fresh ground water may contain elevated oxygen concentrations, that the oxygen is not reduced during flow through the nearshore sediments, and/or the water resides in the sediment for an insufficient time for the oxygen to be reduced.

If fresh ground water interacts with the granitic aquifer material during its flow to discharge points at the seepage face, it would be expected that the major element concentrations and pH (Fig. 10) would reflect those alteration reactions. In granitic terrains, water chemistry can change through incongruent dissolution of alkali feldspars to clay minerals such as kaolinite by the following reactions:

$$2NaAlSi_3O_8(albite) + 2H^+ + 9H_2O \rightarrow Al_2Si_2O_5(OH)_4(kaolinite) + 2Na^+ + 4H_4SiO_4(aq).$$

$$2KAlSi_3O_8(K-feldspar) + 2H^+ + 9H_2O \rightarrow Al_2Si_2O_5(OH)_4(kaolinite) + 2K^+ + 4H_4SiO_4(aq)$$

These reactions consume H^+, which for most terrestrial systems is in the form of carbonic acid (H_2CO_3) resulting from equilibration with atmospheric CO_2. These reactions also release K^+, Na^+, and H_4SiO_4, which is a weak acid with a dissociation constant of $10^{-9.9}$ at 25ºC (Stumm and Morgan, 1996). Fresh water discharging in the Ubatuba region is characterized by low pH values and K/Cl and Na/Cl ratios that are mostly less than seawater values. These characteristics of the water chemistry indicate that its residence time in the aquifer is insufficient for significant alteration of water chemistry through weathering of feldspar minerals, notwithstanding the observed extensive alteration of the solids in the well boring and cores (e.g. Fig. 3). Weathering of the bedrock may have occurred at an earlier time and is not reflected in the modern water chemistry. Alternatively, the water/rock ratio may be sufficiently high in this high precipitation region that weathering proceeds without significant alteration to the water chemistry. A third possibility is that most of the fresh water flows through unaltered sediments but rapidly mixes with and is lost to the overlying seawater. Restriction of the flow to the unaltered material could result from alteration to clay minerals and the associated reduction in permeability forcing water to flow through less altered zones in the aquifer characterized by higher permeability. The higher permeability would also allow mixing between the shallow permeable sediments and the overlying water column that would be produce the elevated salinity that are found in the upper

portions of the multisampler profiles at MS 5 and MS3. (e.g., Martin et al., 2004; Cable and Martin, this volume)

Conclusions

The seepage of freshwater is limited at the site by variations in permeability of the sediments overlying the weathered bedrock, with freshwater discharging through the coarse, nearshore sediments but not from the offshore, fine-grained materials. Freshwater seepage rates average on the order of hundredths of meters per day through the approximately 24 m offshore seepage zone. The oxygen concentrations reflect limited organic matter diagenesis, but nonetheless, the SGD appears to contribute DIN to the overlying water column suggesting the nitrogen has a terrestrial source. Major element chemical composition of the water appears not to reflect alteration of the granitic aquifer although much of the solid material is altered. The lack of alteration may reflect flow through unaltered sediment which is not observed as low salinity values because of mixing between the overlying seawater and the fresh water in the sediment pore spaces.

Acknowledgments

The Intergovernmental Oceanographic Commission of UNESCO provided travel funds that permitted participation in this field experiment. M.C. and M.A. were also supported by grants from the National Science Foundation (OCE-0095384) and the NOAA-CICEET program (NA17OZ2507-03-723).

References:

Burnett, W.C., Chanton, J., Christoff, J., Kontar, E., Krupa, S., Lambert. M., et al., 2002. Assessing methodologies for measuring groundwater discharge to the ocean, EOS 80: 13-15.

Charette, M.A., and K.O. Buesseler, 2004. Submarine groundwater discharge of nutrients and copper to an urban subestuary of Chesapeake Bay (Elizabeth River), *Limnology and Oceanography*, 49, 376-385.

Harvey, J.W., Odum, W.E., 1990. The influence of tidal marshes on upland groundwater discharge to esturaries, *Biogeochemistry*, 10, 217-236.

Hvorslev, M.J., 1951. Time Lag and Soil Permeability in Ground-Water Observations, Bull. No. 36, Waterways Exper. Sta. Corps of Engrs, U.S. Army, Vicksburg, Mississippi, pp. 1-50.

Jacob, C.E., 1950. Flow of Groundwater, in *Engineering Hydraulics*, H. Rouse, ed., John Wiley Sons, New York.

Krest, J.M., W.S. Moore, L.R. Gardner, and J.T. Morris. 2000. Marsh nutrient export supplied by groundwater discharge: Evidence from radium measurements. *Global Biogeochem. Cyc.* 14**:** 167-176.

Martin, J. B., J. E. Cable, P. W. Swarzenski and M. K. Lindenberg, 2004. "Mixing of ground and estuary waters: Influences on ground water discharge and contaminant transport." *Ground Water* 42: 1000-1010.

Martin, J. B., K. M. Hartl, D. R. Corbett, P. W. Swarzenski and J. E. Cable, 2003. "A multilevel pore water sampler for permeable sediments." *Journal of Sedimentary Research* 73: 128-132.

Nuttle, W.K., Harvey, J.W., 1995. Fluxes of water and solute in a coastal wetland sediment, 1. The contribution of regional groundwater discharge, *Journal of Hydrology*, 164, 89-107.

Rebouças, Aldo da C., 2002. Aguas Subterraneas, *Aguas Doces no Brasil*, 2nd Edition, A. Rebouças, B. Braga, and J.G. Tundisi, eds., Escrituras, São Paulo, Brazil.

Robinson, M.A., 1996. A finite element model of submarine ground water discharge to tidal estuarine waters, PhD dissertation, Virginia Polytechnic Institute, 1996.

Staver, K.W., Brinsfield, R.B., 1996. Seepage of groundwater nitrate from riparian agroecosystems into the Wye River Estuary, *Estuaries,* 19:28, 359-370.

Stumm, W. and J. J. Morgan, 1996. *Aquatic Chemistry*. New York, John Wiley and Sons, Inc., 1022 p.

Vanek, V., 1993. Groundwater regime of a tidally influenced coastal pond, *Journal of Hydrology*, 151, 317-341.

Table 1. Hydraulic conductivity (K) values and corresponding fresh SGD.

Method for K determination	**K (m/d)**	**Fresh SGD (m^3/d/m shoreline)**
Slug/bail test on weathered bedrock (well 0)	0.09	0.003
Slug/bail test on beach sand (well 1B)	2.5	0.083
Bail tests on surf zone granitic sands (wells 2A,2B)	0.9 to 2.2	0.03 to 0.07
Bail tests on surf zone sands/fine sediments (wells 3A,3B)	3.3 to 4.5	0.11 to 0.15
Tidal signal propagation	5.3 to 49	0.17 to 1.6

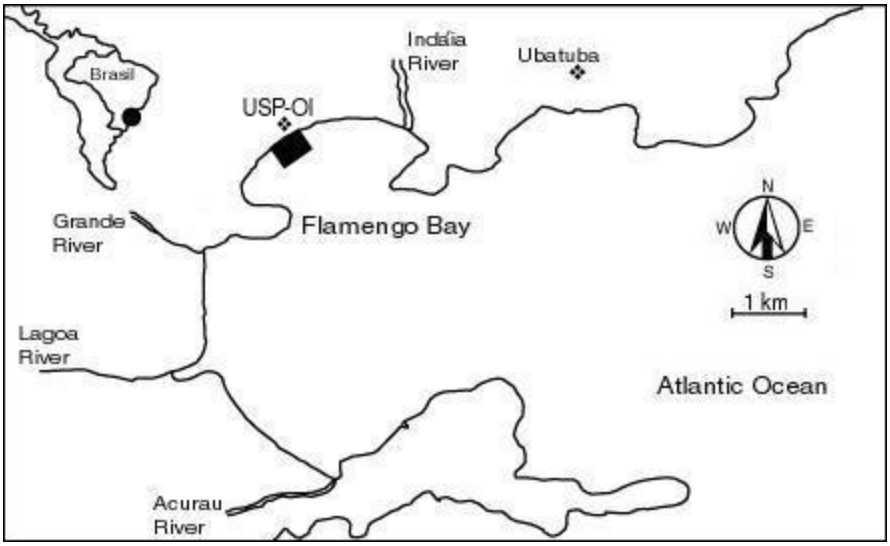

Figure 1. Map showing location of field site at the University of São Paulo Oceanographic Institute.

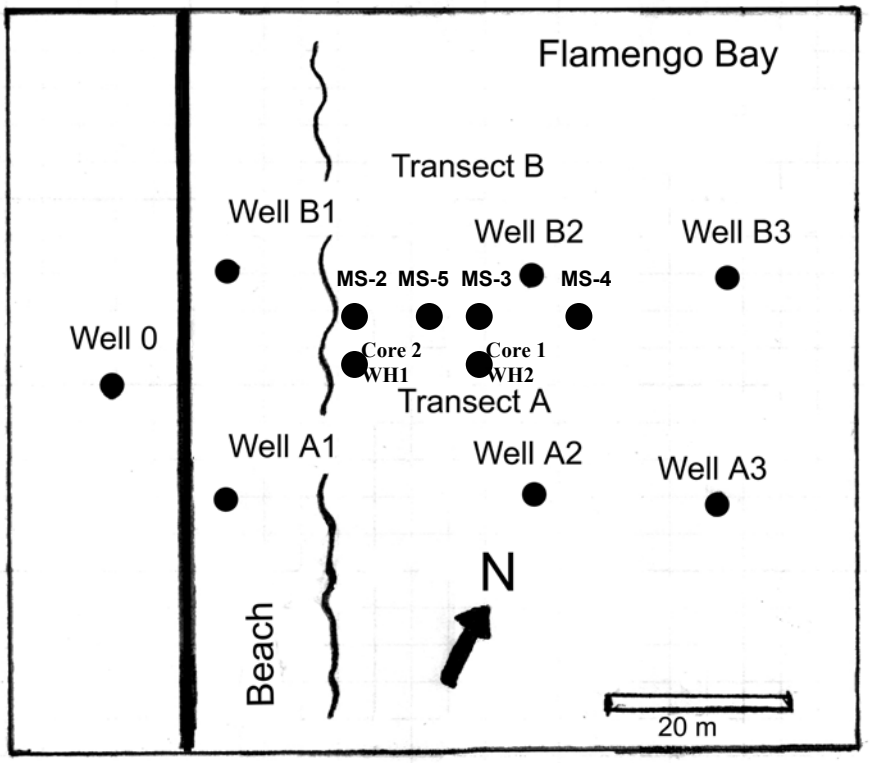

Figure 2. Location map for field installations at University of Sao Paulo Marine Laboratory at Flamengo Bay.

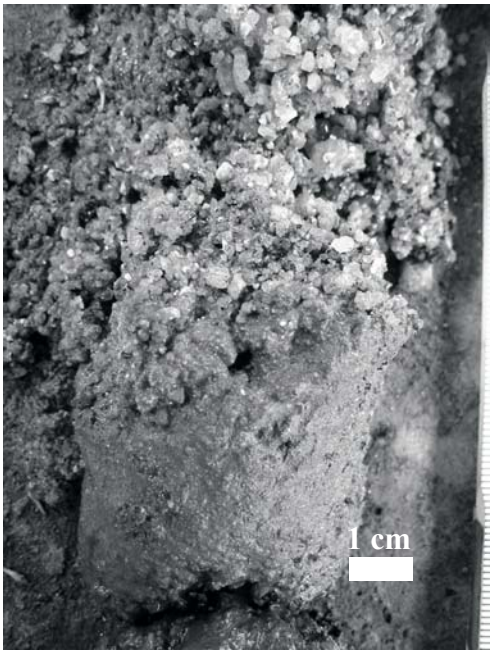

Figure 3. Photograph of core sample showing transition from overlying sand to hard layer atop the weathered bedrdock.

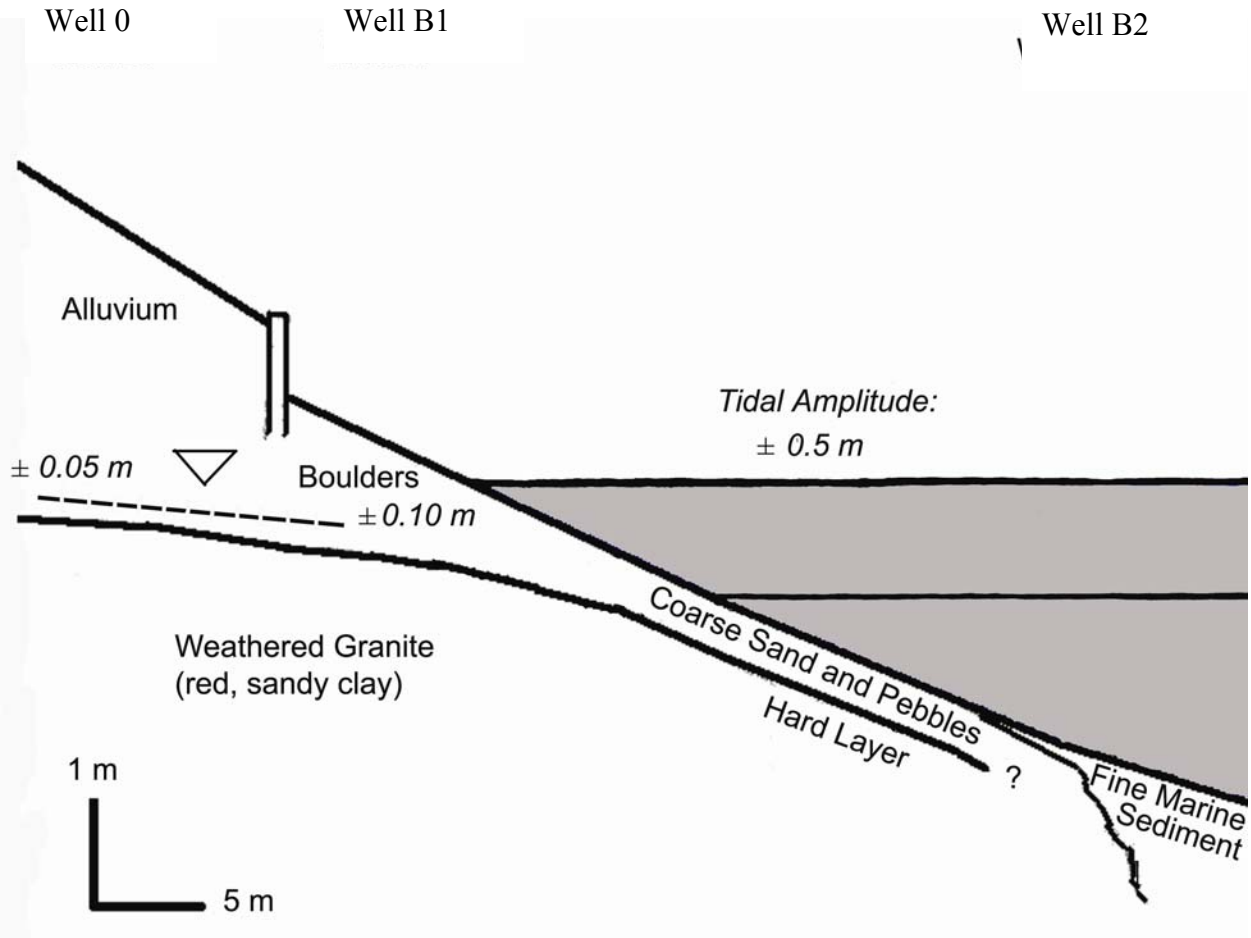

Figure 4. Conceptual model of geology and hydrogeology at transect B.

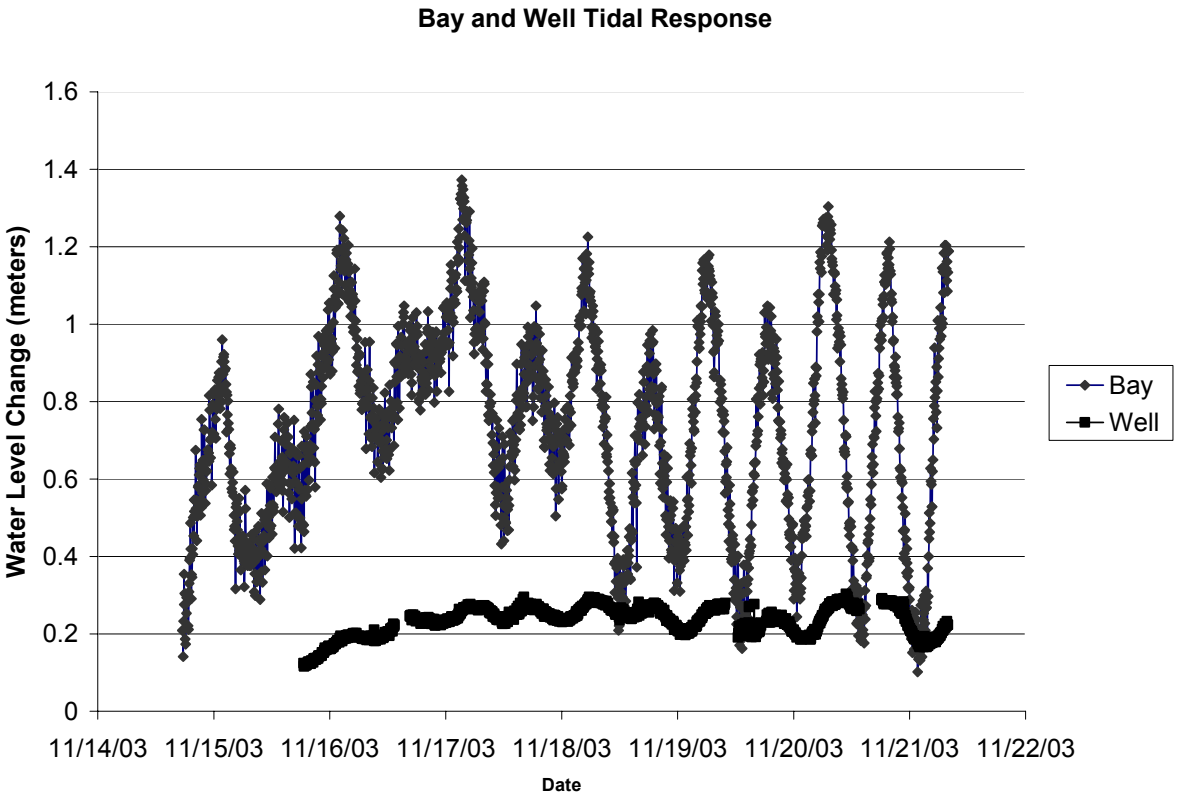

Figure 5. Tidal signal in Flamengo Bay and well 0.

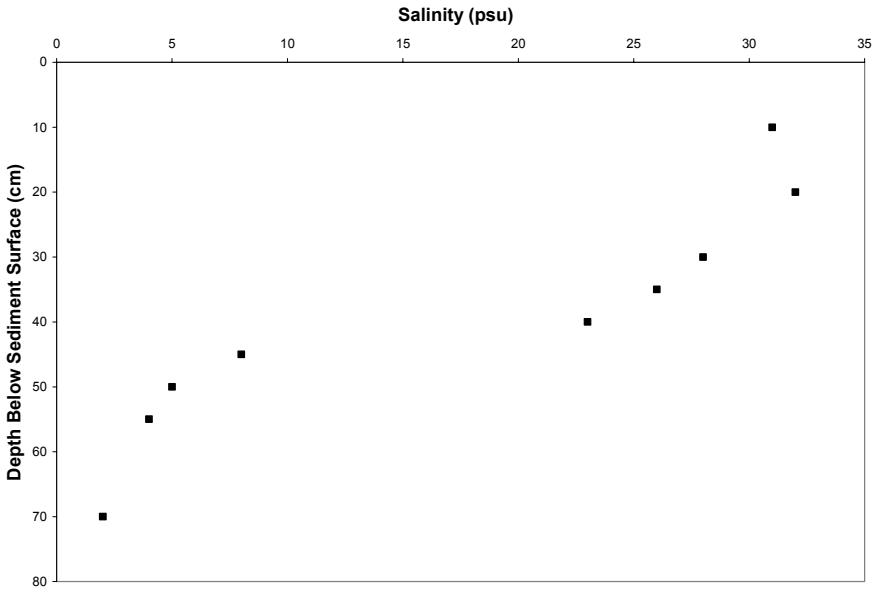

Figure 6. Porewater salinity profile, located 2 m offshore from the high tide line near Transect B and measured at high tide. The hard, fine-grained layer was encountered around 42 cm, corresponding to the abrupt change in salinity.

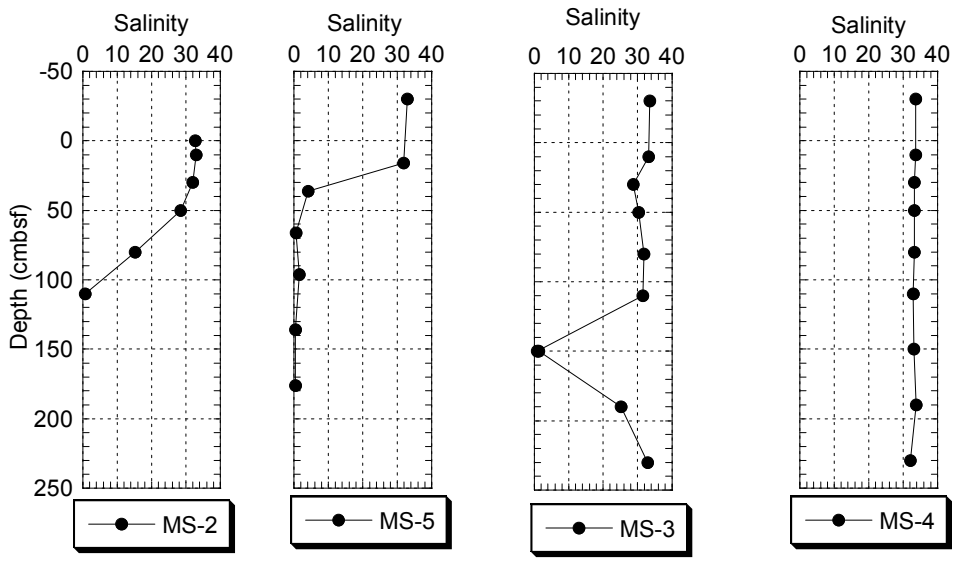

Figure 7. Pore water salinity versus depth in multi-level piezometer transect extending offshore along transect B. Low saline fluid underlies salt water in upper section of sediment. Tongue of fresh water extends offshore to approximately 10.5 m from the low tide line near MS3. Freshwater signal has disappeared from pore waters by about 26 m offshore.

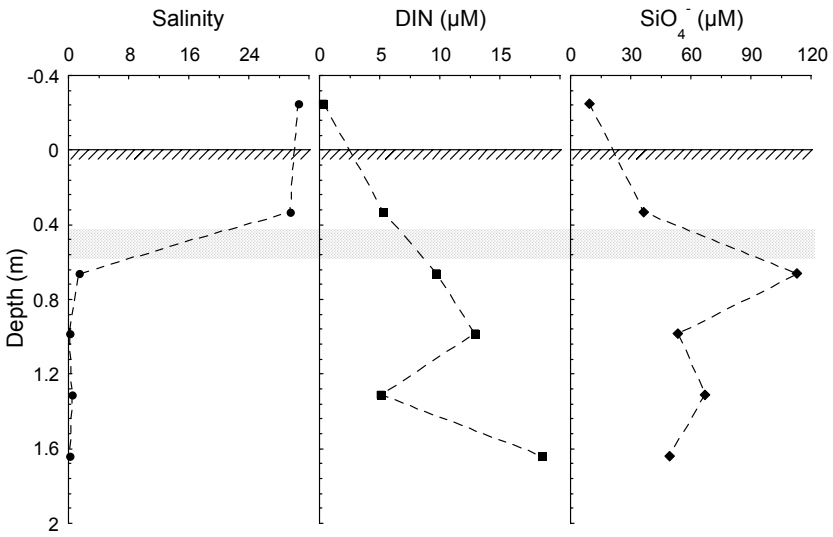

Figure 8a. Nearshore piezometer (WH1) profile of salinity, dissolved inorganic nitrogen, and silicate.The hatched line indicates the sediment water interface; the shaded region is the location of the coarse-fine sediment transition.

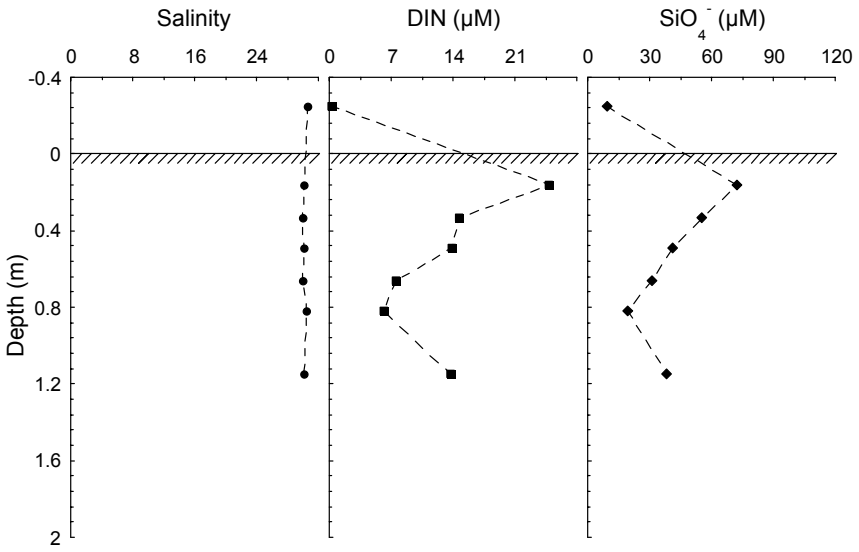

Figure 8b. Offshore piezometer (WH2) profile of salinity, dissolved inorganic nitrogen, and silicate. The hatched line indicates the sediment-water interface.

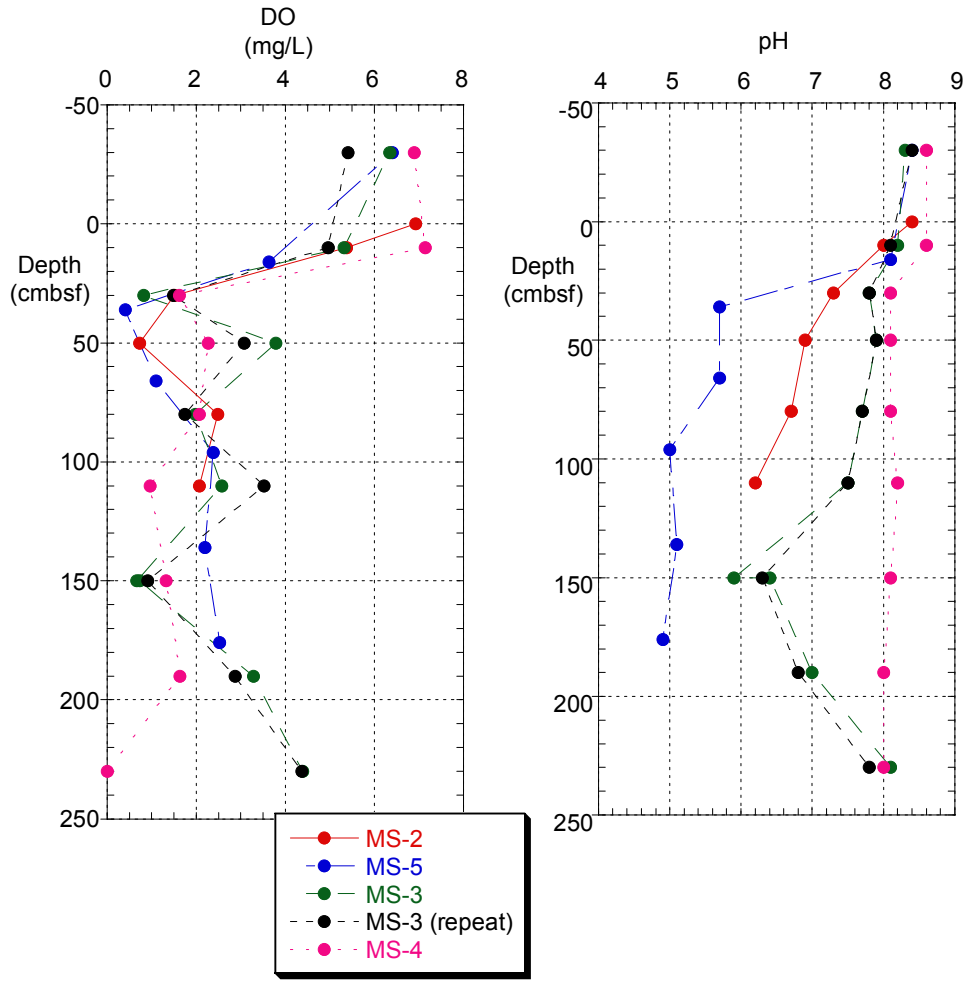

Figure 9. pH and DO versus depth at the four stations of the multi-level piezometers.

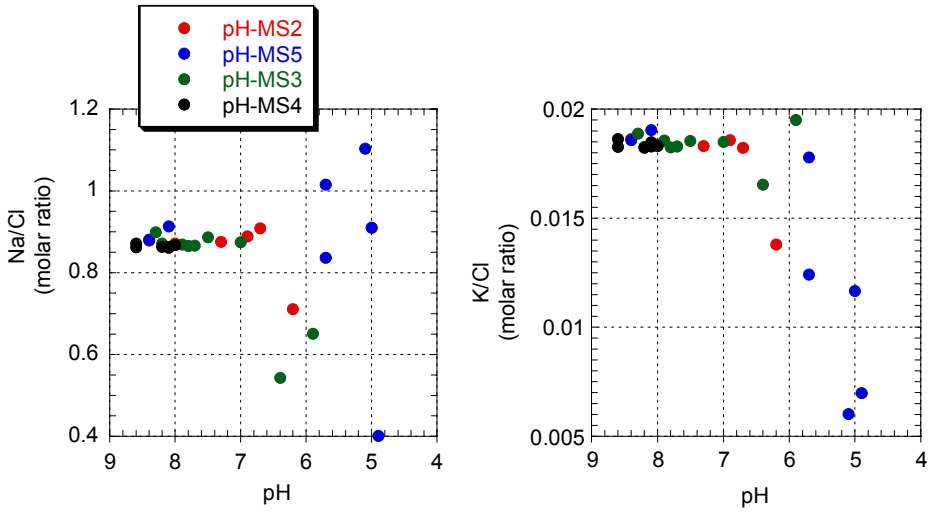

Figure 10. Na/Cl molar ratio and K/Cl molar ratio versus pH for the four multi-level piezometer stations.